BRCORP
TECHNOLOGY | INNOVATION | INDUSTRY

International Journal of
Advanced Structures & Geotechnical Engineering
ISSN 2319-5347, Vol 6, No 3, July-2017

Soil-Structure Interaction Effects on Seismic Behaviour of Base-Isolated Nuclear Power Plants

SHAFAYAT BIN ALI*[1], DOOKIE KIM [2]
[1]*Institute of Earthquake Engineering Research (IEER), Chittagong University of Engg. & Tech, Bangladesh*
[2]*Department of Civil and Environmental Engineering, Kunsan National University, Gunsan, South Korea*
*Corresponding Author *Email: shafayatce@yahoo.com*

Abstract: The soil-structure interaction effects between the structure and its geological medium become important for massive structures such as nuclear power plants. The present study investigates the effects of soil-structure interaction (SSI) on the seismic responses of base-isolated nuclear power plant (NPP). A comparison between seismic performances of the base-isolated NPP and rigidly fixed NPP to the ground is examined considering SSI effects. In this study, a nuclear power plant structure with total height of 65.8m is modelled as a lumped mass stick model and seismic isolation system is adopted by using lead rubber bearing (LRB) isolation device. To incorporate SSI effects the underlying soil medium is assumed as a homogenous half-space and modelled by the concept of cone models. Moreover, two shear wave velocities are used in SSI system to represent the real rock site conditions of NPP structures. The results leading to conclude that the effects of SSI on seismic performances of the base-isolated NPP are negligible than the rigidly fixed NPP rested on rock sites.

Keywords: *Nuclear Power Plant, Base Isolation, Soil-Structure Interaction, Cone model, Seismic Responses*

Introduction:

Seismic isolation systems have been considered as an important concept to protect important structures from risks posed by seismically induced ground motions. Few number of structures with base isolation system have faced significant earthquake forces (Constantinou et al. 2007). Many researchers (Stewart et al. 1999 and Kani et al. 2006) conducted their study to investigate the effectiveness of isolation system under earthquakes. Now a day's many conventional structures like building, bridges, viaduct etc. are designed incorporating seismic base isolation. Nonetheless the application of seismic isolation is quite limited to Nuclear Power Plant Industry. At present only two nuclear power plants (NPPs) are constructed with base isolators, one is located in France with four pressurized water reactors and another is in South Africa (Malushte and Wittaker 2005). Moreover, in France a new base-isolated nuclear reactor is under construction (Forni 2011). Many studies have been done to examine the seismic responses of NPP using base isolators under earthquake forces. Micheli et al. (2004) investigated the behaviour of a special isolating system for Nuclear Island and concluded that the base isolation has major effect in drastic reduction of floor acceleration. A numerical simulation of NPP containment building under three-directional seismic loading has conducted by Zhao and Chen (2013).

Received: March 30, 2017; Submitted with Revision: December 27, 2017; Accepted: January 2, 2018, Published: January 5, 2018
DOI: 10.5281/zenodo.1135358
Cite the Article: Ali, S. B. and Kim, D. (2017). Soil-Structure Interaction Effects on Seismic Behaviour of Base-Isolated Nuclear Power Plants. International Journal of Advanced Structures and Geotechnical Engineering, 6:103–113

Forni et al. (2012) presented the state-of-art of the base-isolated nuclear power plants. Up to date, no specific standards are available for design of base isolated NPPs.

Soil-structure interaction may play significant role under seismic force in altering seismic response of superstructure, especially for massive structures built on relatively soft soil. Usually the effect of SSI on seismic behavior of base-isolated structures is neglected. The studies of SSI effects on the seismic response of structures had begun to take into account seriously after the 1971 San Fernando earthquake. In the 1980s and 1990s, many numerical methods were developed to consider SSI effect in the design of structures (Spyrakos et al. 1986, Gazetas 1991 and Wolf 1994). Novak and Henderson (1989) investigated the SSI effects on the modal properties of base-isolated buildings and proposed that the effects should account for base isolated structures. Chaudhary et al. (2001) have examined the structural and geotechnical parameters of base-isolated bridge considering the SSI phenomena under seismic excitations. A numerical study on a three-span bridge considering SSI effects has carried out by Tongaonkar and Jangid (2003). The study shows that SSI has incremental effects in seismic displacements of bridges. Spyrakos et al. (2009) conducted a study to investigate the SSI effects on the seismic behavior of base-isolated buildings and the finding is that for squat and stiff base-isolated structures SSI has noticeable influence. A numerical simulation of isolated 9-story shear wall is conducted by Song and Ding (2009). They concluded that SSI has significant influences on isolator displacement rather than story drift of the structure. Mahmoud et al. (2012) carried out a research which shows a comparison among the

responses of isolated buildings with and without adopting SSI effects under seismic excitations.
Very few studies have been conducted to investigate the seismic responses of base-isolated nuclear power plant considering soil-structure interaction effect (Kelly 1991). Therefore, additional research is needed on the topic. The present study focuses on investigation of SSI effects on the seismic responses of base isolated NPP structure and compares with rigidly fixed NPP to the ground. In that regard, NPP structures are designed as a lumped mass stick model with and without considering base isolation system. The soil model is adopted using the concepts of cone models. Three different earthquake excitations i.e., 1940 El-Centro, 1989 Loma Prita and 1995 Kobe are applied along the longitudinal direction (X-direction) of the NPP structural models. Dynamic analysis is done by OpenSees navigator compatible with OpenSees platform.

Analytical Model:

Nuclear Power Plant (NPP) Model:

The numerical analysis of the study is conducted by using a typical nuclear power plant, like APR1000, which is a pressurized water reactor (PWR). The total height of the reactor containment building (RCB) is 65.8m. The modelling of NPP structure is done by lumped mass stick model consisting of fourteen nodes and thirteen three dimensional beam elements which is shown in Figure 1 (Lee and Song 1999). The Table 1 presents the corresponding nodes on each element's edge of NPP where the actual translational and rotational masses are transferred. Table 2 exhibits the properties of beam element of NPP model. The NPP structure is designed to have a Safe Shutdown Earthquake (SSE) of 0.3g as a design basis earthquake to increase the ductility against earthquakes (AP1000®, Westinghouse Electric Company 2011 and Jang et al. 2010).

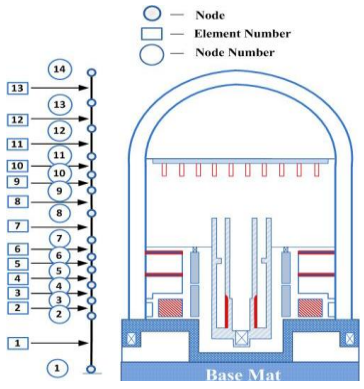

Figure 1: Nuclear Power Plant stick model and containment building

Base Isolator Design:

In the present study seismic isolation system is adopted by using lead rubber bearing (LRB) isolation device. Total 121 isolators are used to provide discontinuity between NPP structure and foundation. The LRB base-isolator consists of low damping natural rubber and a lead plug damper. The device is designed by following the design procedures of the International Organization for Standardization (ISO) (2010). The outer diameter of the isolator is 1950 mm and total height is 350 mm, which consists of 10 rubber layers 18 mm thick. In this study equivalent linear analysis is used to describe the behaviour of isolator. Figure 2 and Table 3 illustrate the equivalent linear properties of the isolator where K_u is the linear horizontal tangential stiffness, K_d is the post-yield horizontal stiffness and K_H is the effective horizontal stiffness. Q_d is the characteristic strength and F_y is the yield strength. The maximum horizontal displacement and the minimum horizontal displacement of the isolator are denoted by δ_{max} and δ_{min} respectively. Moreover F_{max} is the maximum horizontal force and F_{min} is the minimum horizontal force corresponding to the maximum and the minimum displacements of the isolator, respectively.

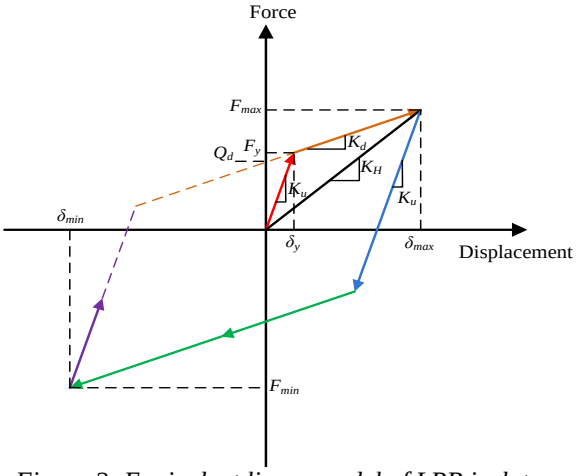

Figure 2: Equivalent linear model of LRB isolator

The total 110,950 tons weight of NPP structure is considered to design the dynamic properties of the isolators. The horizontal stiffness of isolators is calculated by using the following equation:

$$K_t = M\left(\frac{2\pi}{T_H}\right)^2 \quad (1)$$

In the above equation, K_t is the total global horizontal tangential stiffness, M is the total mass of the structure with base mat and T_H is the target fundamental period of structure, which is considered as 2 sec preliminarily. The horizontal stiffness of single isolator is calculated by the following equation:

$$K_H = \frac{K_{total}}{N} \quad (2)$$

Table 1: Characteristics of nodes and lumped masses of the NPP

Node	Height (m)	Translational mass (tonf.sec^2/m)		Rotational mass (tonf.m.sec^2)		
		$M_x = M_y$	M_z	M_{xx}	M_{yy}	M_{zz}
1	0.00	1074.11	1074.11	274145.98	274145.98	548291.95
2	5.18	1916.76	2103.12	481531.58	474277.96	955809.54
3	8.53	1392.11	1392.11	354667.88	354667.88	709335.76
4	11.89	1649.98	1949.45	365514.41	393810.29	759338.25
5	14.94	1265.58	1265.58	322372.35	322372.35	644744.69
6	17.98	1328.63	1977.32	456137.14	415828.74	871965.88
7	21.34	2087.95	2087.95	532984.79	532984.79	1065956.02
8	28.04	3606.73	3606.73	924625.77	924625.77	1849197.31
9	38.71	2847.27	2847.27	725161.10	725161.10	1460349.31
10	41.76	2005.93	2005.93	400968.99	422255.25	823224.25
11	44.81	2011.77	2011.77	499387.67	499387.67	985420.56
12	52.43	2758.83	2758.83	626373.39	626373.39	1225982.97
13	60.05	2758.83	2758.83	393756.05	393756.05	760002.60
14	65.84	1242.96	1242.96	58658.02	58658.02	114280.37

Table 2: Characteristics of beam elements of the NPP

Element	Cross-sectional area (m^2)	Shear area (m^2)	Moment of inertia (m^4) $I_{xx} = I_{yy}$	Polar moment of inertia (m^4)
		$A_x = A_y$	$I_{xx} = I_{yy}$	
1	172.80	86.40	43983.45	87949.63
2	172.80	86.40	43983.45	87949.63
3	172.80	86.40	43983.45	87949.63
4	172.80	86.40	43983.45	87949.63
5	172.80	86.40	43983.45	87949.63
6	172.80	86.40	43983.45	87949.63
7	172.80	86.40	43983.45	87949.63
8	172.80	86.40	43983.45	87949.63
9	172.80	86.40	43983.45	87949.63
10	172.80	86.40	43983.45	87949.63
11	42.36	61.50	25208.41	60425.45
12	42.18	61.22	22992.92	45985.83
13	44.41	64.47	9278.25	18556.60

Table 3: Equivalent linear properties of the LRB base isolator

Horizontal Stiffness	Post-yielding Stiffness	Yield Strength	Characteristic Strength	Yield Displacement	Hardening ratio
K_H (kN/m)	K_d (kN/m)	F_y (kN)	Q_d (kN)	δ_y (mm)	α
8436.10	7089.55	303.73	269.31	4.85	0.113

where K_H is the horizontal (effective) tangential stiffness of the single isolator and N is number of isolators. Total 121 LRB isolators are used in the present study to provide isolation between structure and foundation. The linear horizontal stiffness of the isolator can be represented as $K_u = (4\sim6.5)\times K_H$ which is considered $4\times K_H$ in this study. The yield strength of the isolator can be expressed as F_y = {(0.03~0.05)×total weight of structure} which is taken 0.05 times of total weight of structure for this study. The characteristic strength and hardening ratio of isolator are represented by the equation (3) and (4) respectively.

$$Q_d = F_y\left(1-\frac{K_H}{K_u}\right) \quad (3)$$

$$\alpha = \frac{K_d}{K_u} \quad (4)$$

Base Mat of NPP:

The stick model of NPP containment building rests on a base mat where 121 LRB isolators are used for seismic isolation. The dimensions of the base mat are 100m × 80m. Total thickness of the base mat is 12m under the containment building and 4m for the rest of

the area. In this study OpenSees Navigator is used for modelling the total base-isolated NPP structure (Schellenberg 2013). Figure 3 illustrates the nuclear island base mat dimensions in global axes. Table 4 shows the dimensions of base mat and number of isolators placed in X and Y direction under base mat.

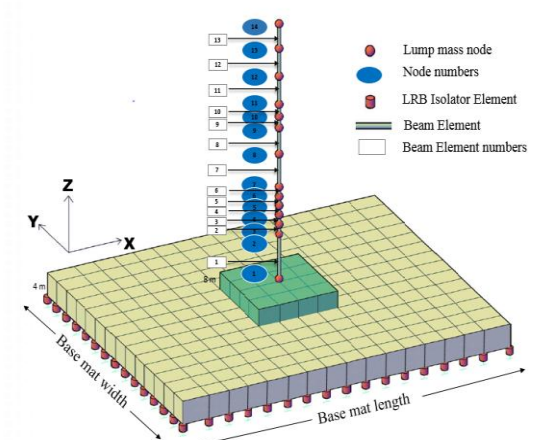

Figure 3: Nuclear island base mat dimensions

Table 4: Dimensions of base mat of BI-NPP model

Base mat dimensions			No. of LRB isolators	
Length (m)	Width (m)	Area (m^2)	along X-dir.	along Y-dir.
100	80	8000	11	11

Soil-Structure interaction:

In this study sub-structure method is used to consider soil-structure interaction effects on seismic response of BI-NPP structure. In this approach the homogenous half-space soil stratum and the structure are modelled independently and then combined together. The modelling of stratum is done by the concept of viscoelastic cone model based on one-dimensional wave propagation. The cone model is proposed by Meek and Wolf (1993a & 1993b) and Wolf (1994). The model is based on the assumptions that the mechanism of soil-structure interaction is obtained approximately by a truncated semi-infinite cone and the superstructure is considered to be rested on a homogenous semi-infinite layer for extracting soil springs and dashpots.

The main geometric property of semi-infinite truncated cone is that the stress distribution area under the basement of structure increases linearly with depth.

$$A = \left(\frac{z}{z_0}\right)^2 A_0 \qquad (5)$$

where A is the stress distribution area of the cone at any depth z and $A_0 = \pi r_0^2$ is the area of the equivalent disk on the surface (Figure 4). The equivalent radius is obtained for the translational modes by equating the area of the rectangular foundation to that of an equivalent disk.

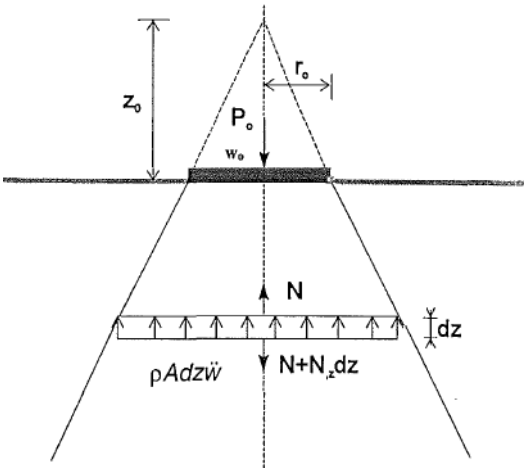

Figure 4: Cone model of soil beneath rigid foundation for translational degree-of-freedom (Wong et al. 1977)

To obtain soil parameter for translational modes of vibration an infinitesimal element of cross-sectional area z and height dz of semi-infinite truncated cone is considered. The element is subjected to an axial force N resulting from a vertical force P_0 acting on the foundation (equivalent disk). The axial displacement from the cone apex due to P_0 is w_0 at the disk and w at any depth z. The static equilibrium condition at the element is represented as:

$$-N + N + \frac{\partial N}{\partial z} dz = 0 \qquad (6)$$

If the element subjected to a harmonic force resulting inertial forces is expressed as:

$$-N + N + \frac{\partial N}{\partial z} dz - \rho A \ddot{w} dz = 0 \qquad (7)$$

By using the force-displacement and constitutive relationships, the following relationship is obtained:

$$N = E_c A \frac{\partial w}{\partial z} \qquad (8)$$

where $E_c = \rho v_p^2$ or $= (2G_s)(1-\upsilon)/(1-2\upsilon)$ which is known as constrained modulus, where ρ is the mass density (kg/m^3), G_s is the elastic shear modulus (N/mm^2), v_p is the dilatational wave velocity (m/s) and υ is Poisson's ratio of the soil.

The wave propagation equation results from substitution of equation 8 into equation 7:

$$\frac{\partial^2}{\partial z^2}(zw) - \frac{1}{v_p^2}\frac{\partial^2}{\partial t^2}(zw) = 0 \qquad (9)$$

If only outwardly propagating waves are considered, the solution of equation 9 is:

$$zw = z_0 f\left(t - \frac{z - z_0}{v_p}\right) \tag{10}$$

where f represents an arbitrary function which is equal to $f(t) = w_0$ when $w(z = z_0) = w_0$ leading to:

$$w = \frac{z_0}{z} w_0\left(t - \frac{z - z_0}{v_p}\right) \tag{11}$$

The first derivative of equation 11 with respect to z (i.e. the strain along the wave path) is:

$$\frac{\partial w}{\partial z} = -\frac{z_0}{z^2} w_0\left(t - \frac{z - z_0}{v_p}\right) - \frac{z_0}{z v_p} w_0'\left(t - \frac{z - z_0}{v_p}\right) \tag{12}$$

where w'_0 is the first derivative of w_0 with respect to the argument $[t-(z-z_0/v_p)]$. Using equation 12 into equation 8 at $z = z_0$ leads to:

$$P_0 = -N(z = z_0) = \frac{\rho {v_p}^2 A_0}{z_0} w_0 + \rho v_p A_0 \hat{w}_0 \tag{13}$$

where $\hat{w} = w'_0\{t-(z-z_0)/v_p\}$ at $z=z_0$. Equation 13 is the force-displacement relationship which is generalized to present both vertical and horizontal components of translational motion as follows:

$$P_0 = \frac{\rho v^2 A_0}{z_0} w_0 + \rho v A_0 \hat{w}_0 \tag{14}$$

or
$$P_0 = k w_0 + c\hat{w}_0 \tag{15}$$

with
$$k = \frac{\rho v^2 A_0}{z_0} \tag{16}$$

and
$$c = \rho v A_0 \tag{17}$$

where k and c are the frequency independent stiffness and radiation damping coefficients of soil, respectively (Ghaffar-Zade and Cahpel 1983). And v is the shear wave velocity for sway and torsional motions and the primary wave velocity for rocking motions. The equation 18 and 19 are used to augment material damping of soil (Wolf 1994).

$$c' = 2\frac{\zeta_0}{\omega_0} k \tag{18}$$

$$m' = \frac{\zeta_0}{\omega_0} c \tag{19}$$

where ζ_0 is the soil's damping ratio and ω_0 is the fundamental frequency of the soil-structure system. Similarly for rotational modes of vibration soil related parameters can be expressed as follows:

$$k_\varphi = \frac{3\rho v^2 I_0}{z_0}, \quad c_\varphi = \rho v I_0, \quad c'_\varphi = 2\frac{\zeta_0}{\omega_0} k_\varphi, \quad m'_\varphi = \frac{\zeta_0}{\omega_0} c_\varphi \tag{20}$$

where I_0 is the moment of inertia of foundation area about the axes of rotation,

In this model four degree of freedoms are considered in x and y directions by permitting sway and rocking motions and one degree of freedom is considered by allowing torsion about z direction. To reflect the rock site conditions of NPP structure two shear wave velocities are used i.e., 600m/s for soft rock and 1000m/s for rock. The other parameters of soil are: $\rho = 2100 kg/m^3$, $\upsilon = 0.4$ (Poisson's ratio) and $\zeta_0 = 0.05$. Figure 5 illustrates the viscoelastic cone model which has been used in this study.

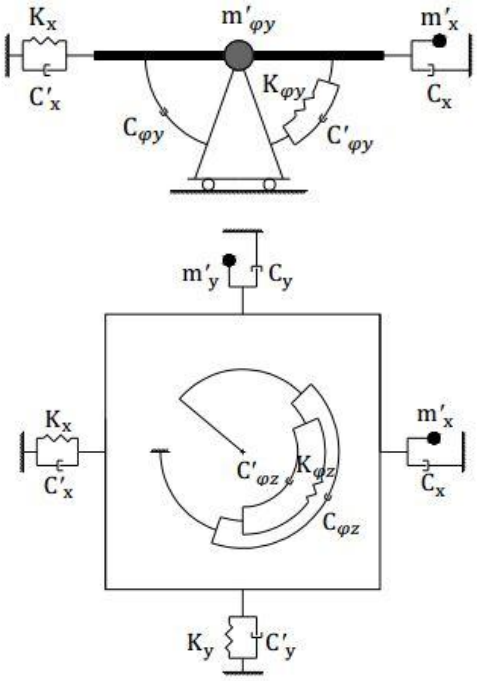

Figure 5: Soil model (Kenarangi and Rofooei 2010)

Results and Discussions:

In this study, to conduct numerical analysis, Newmark-β method is applied with α=0.25 and β=0.50. Moreover, Rayleigh proportional damping is used to consider the damping ratio of the structure. Furthermore, base isolation device is designed with target fundamental period 2 sec. Two analysis cases are defined i.e., the nuclear power plant without base isolator which is called 'NPP' and the base-isolated nuclear power plant which is called 'BI-NPP'. Each analysis case has two subcases, i.e., the fixed base (does not consider the SSI effect) and the flexible base (consider the SSI effect). Two soil conditions that are soft rock (v_s = 600m/s) and rock (v_s = 1000m/s) are used in the SSI model for reflecting the real site conditions of NPP structure.

Three ground motions, i.e., El Centro (1940), Loma Prieta (1989), and Kobe (1995) are applied to obtain the seismic responses for comparison of the seismic behaviors of the structures.

SSI effects on fundamental period:

The dynamic modal analysis is applied to evaluate the SSI effects on fundamental periods of the NPP structures located on two different rock sites. Table 5 illustrates the variation of the fundamental periods of the NPP models. As seen in Table 5 that, the natural period of fixed base NPP is 0.218 sec, which is increased to 0.241 sec when flexible base is considered with soft rock site and 0.224 sec due to rock site. However, when SSI effects are incorporated to BI-NPP model the fundamental period is reached from 2.064 sec to 2.069 sec for soft rock and 2.065 sec for rock site. It can be pointed out that, the consideration of SSI effects causes an increase of the fundamental periods of the nuclear power plant models founded on different rock sites, with and without considering base isolation system.

It is also noticed from Table 5 that, the rate of increase of fundamental period is greater for NPP than BI-NPP when flexible base is considered. The fundamental period of NPP is increased by 10.67% and 2.99% due to the consideration of soft rock and rock site respectively. Moreover, the soft rock has noticeable effect in the increment of fundamental period of NPP structure which is 7.46% than the rock site. However, for BI-NPP model the natural period is increased by 0.26% and 0.09% when the SSI effects are considered as v_s = 600m/s and v_s = 1000m/s respectively, while the natural period is increased by 0.17% for the soft rock than the rock site. Therefore, it can be concluded that, SSI has negligible effects in the increase of fundamental period of BI-NPP structure, however, for the NPP structure the effects are greater. Furthermore, soft rock site has considerable effect on the increment of fundamental period of the NPP structure rather than the BI-NPP structure.

SSI effects on lateral displacement:

The variation of lateral displacement is evaluated in terms of SSI application on the two analysis cases. Table 6 and Figure 6 illustrate the maximum lateral displacements of the NPP and BI-NPP in conjunction with SSI effects. It can be found from Table 6 that, the consideration of SSI on NPP structure is reduced the NPP top displacement by 45.20%, 43.2% due to soft rock and 27.13%, 25.04% due to rock site under El-Centro and Loma Prieta ground motions respectively, while, for Kobe earthquake excitation it is increased by 17.57% and 17.75% for soil with shear wave velocity 600m/s and 1000m/s respectively. The rate of decrease of top lateral displacement is greater, which is about 24% for NPP structure rested on soft rock than rock site for both El-Centro and Loma Prieta ground excitation, whereas for Kobe earthquake it is negligible. However, for BI-NPP structure the top lateral displacement is decreased by 0.36% and 0.09% for El-Centro excitation with soft rock and rock respectively. Whereas the SSI increased the top lateral displacement of BI-NPP by 0.43%, 0.37% for soil with v_s = 600m/s and 0.16%, 0.17% for soil with v_s = 1000m/s, under Loma Prieta and Kobe ground excitations.

It can also be noticed from Figure 6 that when the SSI effects are considered on the NPP structure, the inter story drift (the lateral displacement of NPP stick model top node minus the lateral displacement of bottom node) is decreased dramatically by 53.32%, 46.7% for soft rock and 30.62%, 26.73% for rock site under El-Centro and Loma Prieta ground motions respectively. Moreover, for Kobe earthquake the inter story drift is increased by 6.02% and 12.67% for two rock sites respectively. Furthermore, the decrease rate of story drift is noticeable for NPP structure embedded on soft rock rather than rock site, which is around 30% for both El-Centro and Loma Prieta excitation, whereas it is not significant for Kobe excitation. On the other hand, the change of story drift is minor when the BI-NPP structure is rested on the rock sites. As seen from Figure 6 that when El-Centro and Kobe ground motions are applied the story drift is reduced by 4.52%, 6.19% for soil with v_s = 600 m/s and 4.16%, 1.44% for soil with v_s = 1000 m/s respectively; while for the Loma Prieta earthquake the story drift is increased by 0.92% and 0.37% for two rock sites. Moreover, for BI-NPP structure the effect of softness of rock on the change rate of story drift is negligible. The results conclude that, for BI-NPP structure SSI has no noticeable effects on variation of the lateral displacement and inter story drift under different ground excitations whereas the effects on the NPP structure is relatively more considerable. In addition, the changing rate of lateral displacement is prominent for NPP structure when the soil is soft rock.

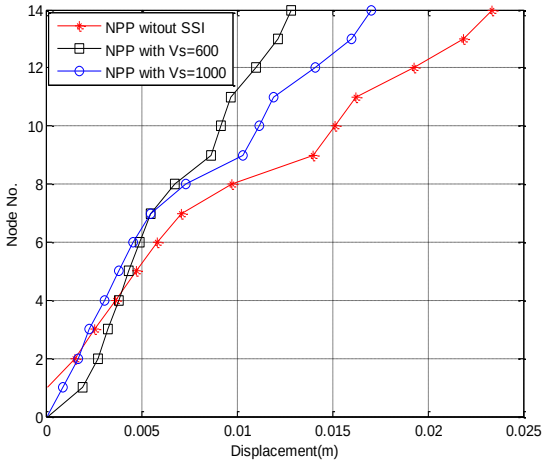

(a) NPP under El-Centro ground motion

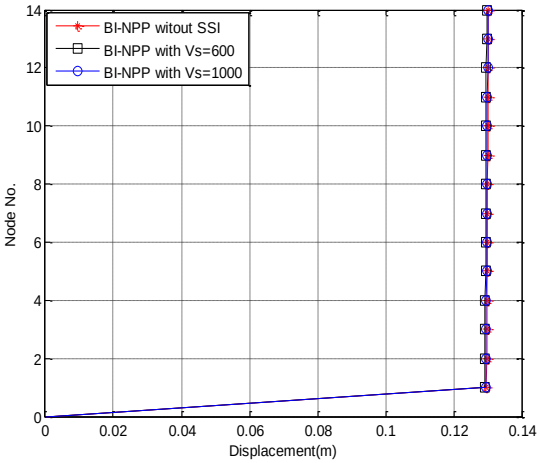

(b) BI-NPP under El-Centro ground motion

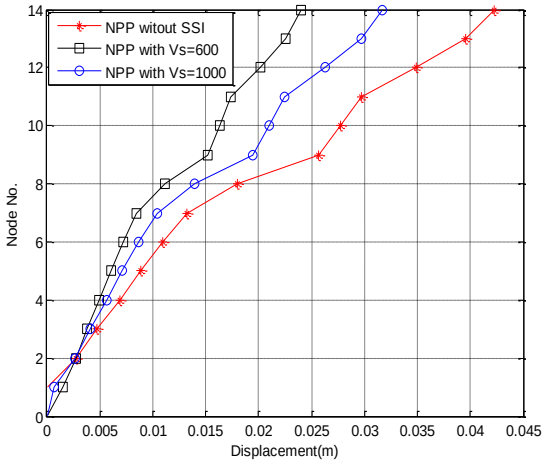

(c) NPP under Loma Prieta ground motion

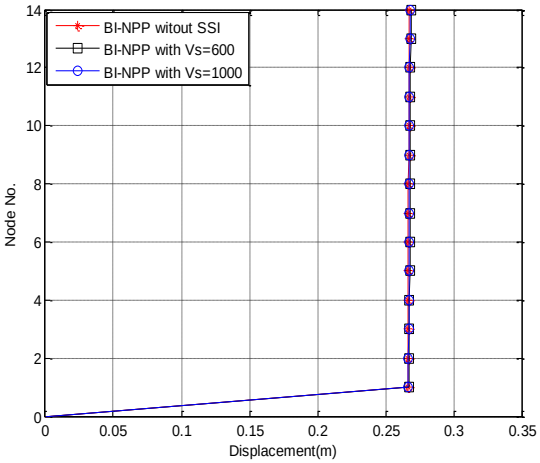

(d) BI-NPP under Loma Prieta ground motion

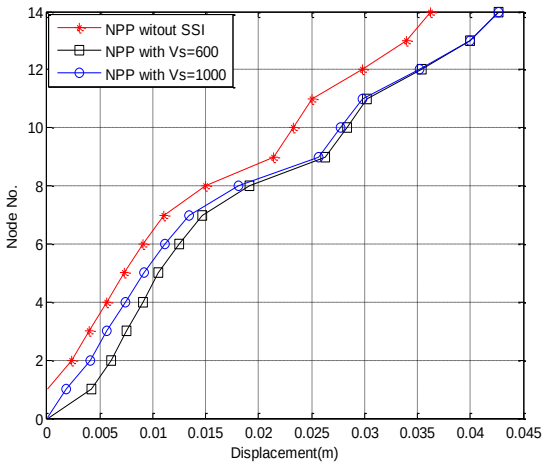

(e) NPP under Kobe ground motion

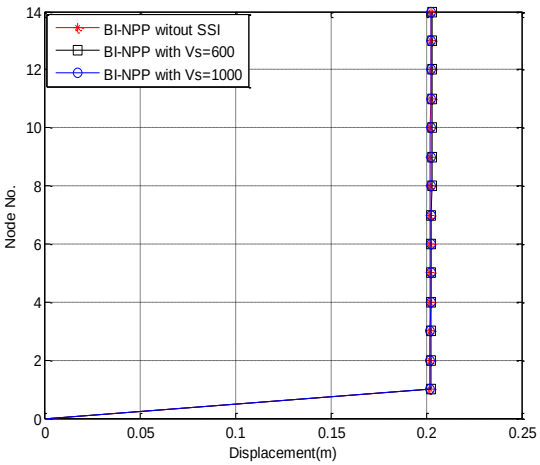

(f) BI-NPP under Kobe ground motion

Figure 6: Maximum lateral displacements of nuclear power plant models

Table 5: Fundamental natural periods of nuclear power plant models

Analysis case	NPP			BI-NPP		
	Fixed base	Flexible base with v_s = 600m/s	Flexible base with v_s = 1000m/s	Fixed base	Flexible base with v_s = 600m/s	Flexible base with v_s = 1000m/s
Fundamental period (sec)	0.218	0.241	0.224	2.064	2.069	2.065

Table 6: Maximum lateral displacements of the top node of nuclear power plant models

Earthquake motion	Maximum lateral displacement (m)of top node					
	Analysis case					
	NPP			BI-NPP		
	Fixed base	Flexible base with v_s = 600m/s	Flexible base with v_s = 1000m/s	Fixed base	Flexible base with v_s = 600m/s	Flexible base with v_s = 1000m/s
El-Centro	0.0233	0.0128	0.0170	0.1302	0.1297	0.1300
Loma Prieta	0.0422	0.0239	0.0316	0.2674	0.2686	0.2678
Kobe	0.0362	0.0426	0.0427	0.2023	0.2031	0.2027

SSI effects on shear force:

The sensitivity of shear forces is investigated for both NPP and BI-NPP models considering SSI effects. Figure 7 illustrates the change of shear forces along the stick model of structure. Figure 7(a) shows that under El-Centro ground motion the shear force of NPP model at node 1 is 275115kN which is decreased to 146069kN and 194699kN for soft rock and rock site respectively and at node 14 it is below 25000kN for both fixed base and flexible base NPP. In Figure 7(c) similar trend is obtained under Loma Prieta ground excitation for NPP model where node 1 has 528754kN shear force which is reduced to 290741kN for soft rock and 392127kN for rock site. And at top node of the structure shear force is around 50000kN with and without considering SSI effect. But for Kobe earthquake, shear force of NPP structure is concentrated around 450000kN at node 1 and 40000kN at node 14 for fixed base and flexible base with considering SSI effect. For BI-NPP models changes of shear forces are negligible. Figure 7 (b), (d) and (f) represent that the base shear of BI-NPP is around 13000kN, 18000kN and 15000kN and shear force is 800kN, 1000kN and 900kN at top node for El-Centro, Loma Prieta and Kobe earthquakes respectively. As seen in the Table 7, the application of SSI on the NPP models results in decrease of base shear by 46.9%, 45.02% for soil with v_s = 600m/s and 29.23%, 25.84% when soil type has been changed to rock with v_s = 1000m/s under El-Centro and Loma Prieta ground excitations respectively. Further, for the Kobe earthquake the base shear is increased by 3.81% and 7.21% with two types of rocks for NPP model. In addition, the rate of increase of base shear is about 25% for both El-Centro and Loma Prieta ground motions and 3% for Kobe ground excitation, when the underlying soil is changed from rock to soft rock. Whereas no significant change is noticed in the base shear of BI-NPP structure when the SSI effects are considered. Table 7 implies that for El-Centro excitation the base shear of BI-NPP is increased by 1.43% and 0.58% for soft rock and rock respectively while, the decrement of base shear is noticed 0.14%, 0.21% for Loma Prita and 1.32%, 0.46% for Kobe ground motions for soft rock and rock respectively beneath the BI-NPP structure. Moreover, the change rate of maximum base shear for soft rock soil is less than 1% for BI-NPP structures under three ground excitations. Therefore, the results indicate that the consideration of SSI of the BI-NPP structure has negligible effect in the change of base shear forces. Conversely, for NPP structure the SSI has considerable effects to alter the base shear forces. Moreover, the rate of reduction of base shear of NPP structure is increased for soft rock soil.

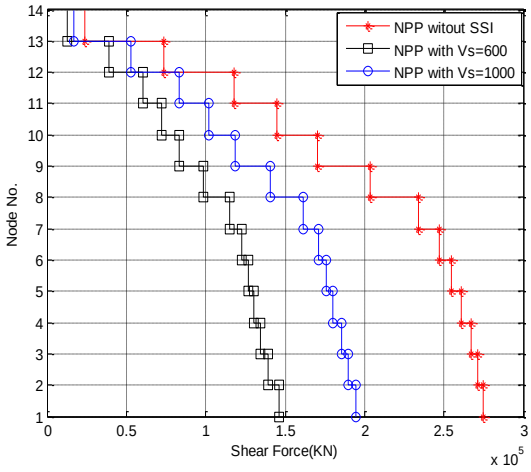

(a) NPP under El-Centro ground motion

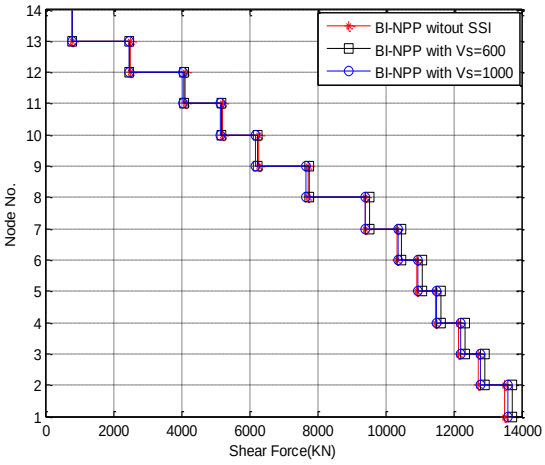

(b) BI-NPP under El-Centro ground motion

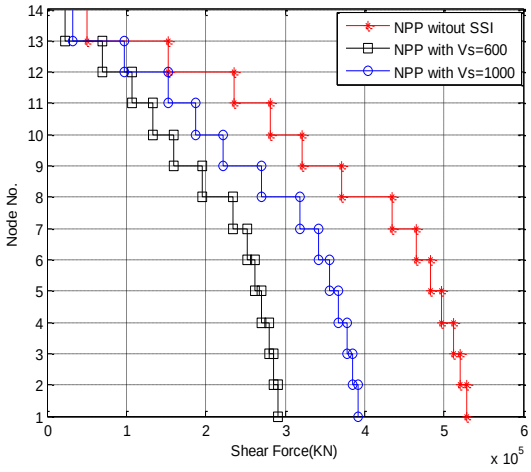

(c) NPP under Loma Prieta ground motion

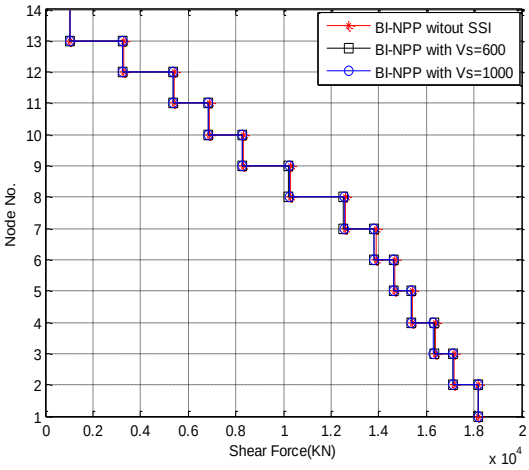

(d) BI-NPP under Loma Prieta ground motion

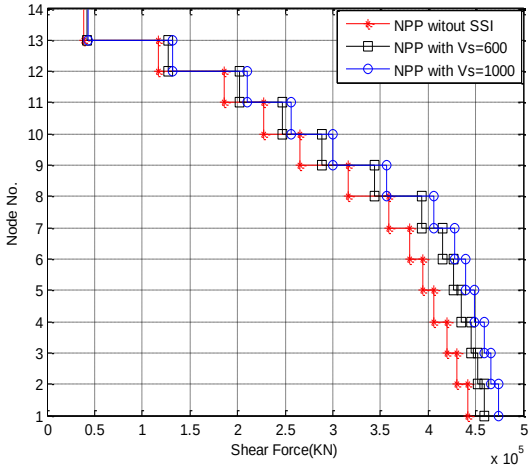

(e) NPP under Kobe ground motion

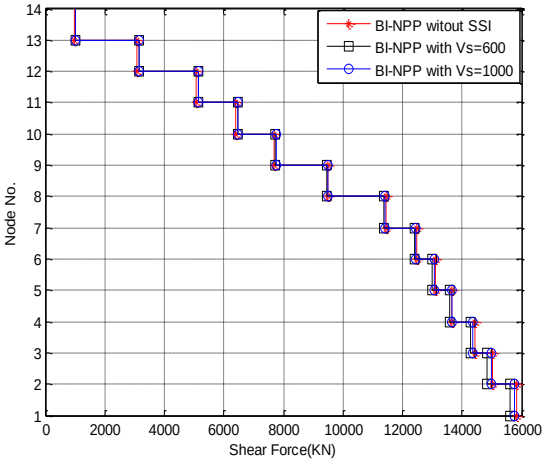

(f) BI-NPP under Kobe ground motion

Figure 7: Shear forces of Nuclear power plant models

Table 7: Maximum base shear forces of nuclear power plant models

Earthquake motion	Maximum base shear forces (kN)					
	Analysis case					
	NPP			BI-NPP		
	Fixed base	Flexible base with v_s = 600 m/s	Flexible base with v_s = 1000 m/s	Fixed base	Flexible base with v_s = 600 m/s	Flexible base with v_s = 1000 m/s
El-Centro	275115	146069	194699	13515.7	13709.9	13593.5
Loma Prieta	528754	290741	392127	18197.2	18172.0	18159.1
Kobe	441791	458627	473641	15828.2	15618.9	15754.6

Conclusions:

The present work investigates the soil-structure interaction effects on seismic behavior of nuclear power plant structure supported on hysteretic bilinear base isolators which rests on a visco-elastic half-space representing the soil. The foundation stiffness and damping coefficients are assumed to be frequency-independent. The results of the analysis and parametric study reveal the importance of SSI on the Nuclear power plant structures. The results show that SSI effects cause an increase of fundamental period of both NPP (without adopting base isolation) and BI-NPP (with adopting base isolation) structures that are rested on soft rock and rock sites. Particularly, for NPP structure on soft rock site, the SSI has a tangible influence on the rate of increase of fundamental period. It also concluded that, SSI has no significant effects on the variation of the lateral displacement or inter story drift for BI-NPP structure; conversely, the effects are greater for NPP structure. Moreover, when the NPP structure rests on soft rock site the rate of change of the lateral displacement is prominent. Furthermore it demonstrates that the consideration of SSI of BI-NPP structure has negligible effects in the change of peak base shear under the different ground motions. However, for NPP structure the effects are more considerable. Furthermore, the reduction rate of base shear is noticeably increased for NPP structure embedded on soft rock for the applied earthquakes.

The findings of the study provide a clear relationship between SSI effect and seismic response of Nuclear power Plant Structures. It is concluded that horizontal responses of BI-NPP structure are not sensitive to soil profile. But the vertical responses of structure may be affected by SSI effect which is not considered in this study. As remarks, it is to emphasize that coupled horizontal and vertical acceleration should be considered to obtain more accurate seismic performance of BI-NPP with considering SSI effect.

Acknowledgment:

This work was supported by the Nuclear power Core Technology Development Program of the Korea Institute of Energy Technology Evaluation and Planning (KETEP) grant financial resource from the Ministry of Trade, Industry & Energy, Republic of Korean (No. 2014151010170A).

References:

AP1000® Nuclear Power Plant Response to External Hazards (2011). *Westinghouse Electric Company LLC*, Non-Proprietary Class 3.

Chaudhary, MTA., Abe´, M. and Fujino, Y. (2001). Identification of soil–structure interaction effect in base-isolated bridges from earthquake records. *Soil Dynamics and Earthquake Engineering, 21(8)*, 713–25.

Constantinou, M.C., Wittaker, A.S., Kalpakidis, Y., Fenz, D.M. and Warn, G.P. (2007). Performance of seismic isolation hardware under service and seismic loading. *Technical Report MCEER-07-0012*, Multidisciplinary Center for Earthquake Engineering Research, State University of New York, Buffalo, New York, USA.

Forni, M. (2011). Seismic isolation of nuclear power plants. *Contribution to the "Italy in Japan 2011" Initiative Science, Technology and Innovation*, 1-8.

Forni, M., Poggianti, A. and Dusi, A. (2012). Seismic isolation of nuclear power plants. *Proceedings of the 15th World Conference of Earthquake Engineering, paper no. 1485*, Lisbon, Portugal, September.

Gazetas, G. (1991). Foundation vibrations. Foundation engineering handbook, 2nd Edition, H.Y. Fang, Ed., *Van Nostrand Reinholds, Chapter 15*, 553–593.

Ghaffar-Zade, M. and Cahpel, F. (1983). Frequency-independent impedance of soil-structure system in horizontal and rocking modes. *Earthquake Engineering and Structural Dynamics, 11*, 523-540.

International Standard Organization (ISO) (2010). Elastomeric seismic-protection isolators-part 3: Applications for buildings-specifications. ISO 22762–3:2010.

Jang, J. B., Lee, Y. and Jang Y. S. (2010). Seismic analysis conditions of APR1000. *Transactions of the Korean Nuclear Society Spring Meeting Pyeongchan*g, Korea, May 27-28.

Kani, N., Takayama, M. and Wada, a. (2006). Performance of seismically isolated buildings in Japan. *Proceedings of the 8th US national*

Conference of Earthquake Engineering, paper no. 2181, San Francisco, CA, USA, April.
Kelly, J.M. (1991). Shake table tests of long period isolation system for nuclear facilities at soft soil sites. *UBC/EERC-91/03*, University of California at Berkeley.
Kenarangi, H. and Rofooei, F. R. (2010). Application of tuned mass dampers in controlling the nonlinear behaviour of 3-D structural models, considering the soil-structure interaction. *Proceedings of the 5th National Congress on Civil Engineering*, Mashhad, Iran, May.
Lee, N.H. and Song, K.B. (1999). Seismic capacity evaluation of the prestressed/reinforced concrete containment, Young-Gwang nuclear power plant units 5 & 6. *Nuclear Engineering and Design, 192*, 189-203.
Mahmoud, S., Austrell, P. and Jankowski, R. (2012). Simulation of the response of base-isolated buildings under earthquake excitations considering soil flexibility. *Earthquake Engineering and Engineering Vibration, 11(3)*, 359-374.
Malushte, S. and Wittaker, A.S. (2005). Survey of past base isolation applications in nuclear power plants and challenges to industry/regulatory acceptance. *Proceedings of 18th International Conference on Structural Mechanics in Reactor Technology, SMiRT 18*, Beijing, China, August.
Meek, W. and Wolf, J.P. (1993a). Cone models for nearly incompressible soil. *Earthquake Engineering and Structural Dynamic, 22(8)*, 649-663.
Meek, W.J. and Wolf, J.P. (1993b). Why cone model represents the elastic half space. *Earthquake Engineering and Structural Dynamic, 22(9)*, 759-771.
Meek, W.J. and Wolf, J.P. (1994). Material damping for lumped-parameter models of foundations. *Earthquake Engineering and Structural Dynamic, 23*, 349-362.
Micheli, I., Cardini, S., Colaiuda, A. and Turroni, P. (2004). Investigation upon the dynamic structural response of a nuclear plant on a seismic isolating devices. *Nuclear Engineering and Design, 228*, 319-343.
Novak, M., Henderson, P. (1989). Base-isolated buildings with soil-structure interaction. *Earthquake Engineering and Structural Dynamic, 18*, 751-765.
Schellenberg, A., Yang, T.Y. and Kohama, E. (2013). *OpenSees Navigator 2.5.2*, https://nees.org/resources/osnavigator.
Spyrakos, C.C. and Beskos, DE. (1986). Dynamic response of flexible strip-foundations by boundary and finite elements. *Soil Dynamics and Earthquake Engineering, 5(2)*, 84–96.
Spyrakos, C.C., Koutromanos, I.A. and Maniatakis, Ch.A. (2009). Seismic response of base-isolated buildings including soil-structure interaction. *Soil Dynamics and Earthquake Engineering, 29*, 658-668.
Song, Z. and Ding, N. (2009). The Analysis of Seismic Responses for Base-Isolated Structures by LS-DYNA. *Science and Technology University of Suzhou*, China.
Stewart, J.P., Conte, J.P. and Aiken, I.D. (1999). Observed behaviour of seismically isolated buildings. *Journal of Structural Engineering, ASCE, 125(9)*, 955-964.
Tongaonkar, NP. and Jangid, RS. (2003). Seismic response of isolated bridges with soil–structure interaction. *Soil Dynamics and Earthquake Engineering, 23(4)*, 287-302.
Wolf, JP. (1994). Foundation vibration analysis using simple physical models. *New Jersey, Prentice-Hall, Englewood Cliffs, NJ*.
Wong, H.L., Luco, J.E. and Trifunac, M.D. (1977). Contact stresses and ground motion generated by soil-structure interaction. *Earthquake Engineering and Structural Dynamics, 5*, 67-79.
Zhao, C. and Chen, J. (2013). Numerical simulation and investigation of the base isolated NPPC building under three-directional seismic loading. *Journal of Nuclear Engineering and Design, 265*, 484-496.